# Power-Over-Fiber Impact and Chromatic-Induced Power Fading on 5G NR Signals in Analog RoF

Rubén Altuna, J. D. López-Cardona, Fahad M. A. Al-Zubaidi, D. S. Montero, and Carmen Vázquez, *Senior Member, IEEE*

***Abstract*—In this work, we investigate the feasibility of optical powering in coexistence with radio transmission using baseband signals with 5G New Radio (5G NR) numerology with different bandwidths (BW) on Analog Radio over Fiber (ARoF) systems with single mode fibers (SMF). We focus on the impact of chromatic dispersion (CD), non-linear effects, High Power Laser (HPL) instabilities and their interactions, performing simulations and experiments. First, without Power over Fiber (PoF), we verify that increasing the BW of the 5G NR baseband signal reduces the CD-induced power fading at the critical RF frequency with the highest extinction and the error-vector magnitude (EVM) of the received 5G NR signal worsens. The CD-induced power fading is 10 dB smaller for 100 MHz versus 10 MHz baseband signal BWs. Then, we experimentally demonstrate the influence of a PoF signal, generated by a Raman HPL, on the transmission of 5G NR signals in a shared scenario with co-transmission of both PoF and data signals. The CD-induced power fading at the critical RF frequency with the highest extinction is 27 dB smaller for 5G NR signal BWs of 10 MHz and 100 MHz respectively when the HPL is set to +33 dBm. This PoF signal enhances the EVM of the received 5G NR signal to values in compliance with the standard while providing an On/Off Raman gain of 12.7 dB at 1552.8 nm data signal in a 14.43 km SMF link. For a 5G NR signal BW of 10 MHz and a RF carrier frequency of 17 GHz, the EVM improves from 31.3% to 11.6% for a HPL power of +33 dBm. For shorter distances such as 100 m, HPL noise transfer does not affect the EVM of data signal.**

***Index Terms*—Analog radio over fiber, chromatic dispersion, 5G-new radio, microwave photonics, non-linear effects, power over fiber.**

## I. Introduction

THE fifth-generation (5G) wireless technology deployment relies on the 5G New Radio (NR) radio access technology developed by the 3rd Generation Partnership Project (3GPP), with key features to allow the promised 10–100X data rate improvement compared with its predecessor, the fourth generation (4G) [1]. 5G-New Radio is constantly evolving and 5G advanced demanding requirements in terms of capacity and energy efficiency are triggering the evolution of new network architectures and new data transmission techniques. To that respect, similar to mobile networks, fixed networks entered their 5th generation (F5G) around year 2020. With the fiber-to-everywhere vision, F5G aims to transform how people and machines communicate in the 5G era [2]. The sixth-generation (6G) mobile technology, which anticipates providing 1 Tbps data rates and ultralow latency over ubiquitous 3D coverage areas, also requires a high capacity transport network able to connect hundreds of thousands of cell sites [3].

Although there are different network architectures in 5G Radio Access Networks (RAN), one of the main architectures proposed for 5G is the cloud/centralized RAN (C-RAN) where the wireless signal processing is centralized in a Base Band Unit (BBU), which is placed at a Central Office (CO). In this architecture, only the antennas are placed at the cell site, which is called the Radio Remote Head (RRH). The fronthaul link connects the pool of BBUs and the RRH. This architecture, in contrast to Distribute Radio Access Networks (D-RAN), enables 5G networks with centralized data processing thus reducing power consumption along with a reduction in the number of BBUs and related cost [4]. The typical fronthaul network operates on a Common Public Radio Interface over optical links, which is a digital radio over fiber technology that requires a larger bandwidth than the alternative Analog Radio Over Fiber (ARoF) technology [1]. ARoF links in C-RAN can achieve high fronthaul data throughput without compromising energy efficiency and with a good scalability [5]. Those fronthaul networks can use the existing Single Mode Fiber (SMF) infrastructure.

Additionally, SMFs offer the possibility to include other functionalities in the fronthaul segment. For example, SMFs can be used to transmit high-power optical signals to feed some parts of 5G NR ARoF networks, e.g., low power RRHs or Radio Frequency (RF) amplifiers therein [6]. This technique is called Power over Fiber (PoF), and has been integrated with RoF transmission in C-RAN based on SMFs [7], [8], Multicore Fibers (MCF) [9], [10], [11], Multimode Fibers (MMF) [12], [13], Double-Clad Fibers (DCF) [14], and in Plastic Optical Fiber (POF) for in home-network scenarios [15].

The use of SMF in 5G NR ARoF networks entails some impairments that need to be tackled. The first one is the Chromatic Dispersion (CD), which leads to a degradation of the received

Manuscript received 31 March 2022; revised 7 June 2022 and 7 September 2022; accepted 7 September 2022. Date of publication 12 September 2022; date of current version 21 October 2022. This work was supported in part by the Ministerio de Asuntos Económicos y Transformación Digital European Union– NextGenerationEU under Grant TSI-063000-2021-135, in part by the Agencia Estatal de Investigación-Ministerio de Ciencia e Innovación under Grants RTI2018-094669-B-C32 and PID2021-122505OB-C32, and in part by the Comunidad de Madrid-Consejería de Educación e Investigación under Grant Y2018/EMT-4892. *(Corresponding author: Carmen Vázquez.)*

The authors are with the Electronics Technology Department, Universidad Carlos III de Madrid, 28911 Leganés, Spain (e-mail: raltuna@pa.uc3m.es; julopezc@ing.uc3m.es; 100386857@alumnos.uc3m.es; dsmontero@ing.uc3m.es; cvazquez@ing.uc3m.es).

Color versions of one or more figures in this article are available at https://doi.org/10.1109/JLT.2022.3205743.

Digital Object Identifier 10.1109/JLT.2022.3205743

data or power fading that depends mainly on the link length and the RF carrier frequency. There are different techniques to overcome chromatic-induced power fading: with compensation techniques using chirped fiber gratings or CD compensation fibers, with optical single sideband (SSB) modulation by using a two-electrode Mach–Zehnder modulator or by eliminating one of the sidebands with an optical filter or using optical phase conjugation [16]. Anyhow, those compensation techniques imply a more complex set-up. Moreover, when a PoF signal is included in the network sharing the optical fiber with the data signal (shared scenario), the PoF signal can give rise to non-linear effects that may damage the data signal quality. Moreover, the High Power Lasers (HPL) used as PoF sources may suffer from some instabilities, especially if fiber lasers are considered. In the power scaling of monolithic fiber lasers, the non-linear effects and transverse mode instability are main limitations. Sometimes tapered gain fibers with longitudinally varying mode area mitigate the non-linear effects but then transverse mode instabilities can appear [17]. As a result, a full characterization of such sources is of great importance. This analysis is important when using high power levels of several W or more. At certain link lengths in the shared scenario, it becomes relevant the noise transfer from the PoF optical source to the data signal.

Hence, this work intends to study the feasibility of remote optical powering in coexistence with radio transmission using baseband signals following 5G NR numerology, with different bandwidths and over SMF ARoF while focusing on the impact of HPL instabilities, the chromatic-induced power fading and their interactions. To that respect, we consider for the first time:

- the impact on ARoF links of chromatic dispersion through power fading for different modulation formats in compliance with 5G NR signals (including baseband bandwidths and subcarrier spacing) and demonstrating through simulations and experimentally that increasing the baseband bandwidth of 5G NR signals reduces the induced power penalty.
- the combination of PoF and its impact on power fading from the perspective of looking for good quality 5G NR mobile signal transmission and the energy delivery. We propose the need of analyzing the noise characteristics of the HPL to identify specific noisy power levels and demonstrate that can be relevant for links longer than several kilometers. Using PoF as a precursor of non-linear effects that counter react ordinary CD, identifying PoF power values that provide an improvement on the quality of the transmitted signal. Verifying that all this is possible without penalizing the efficiency of the PoF system.

For doing so, a summary of the main theoretical concepts regarding non-linear effects, noise transfer and CD-induced power fading in ARoF systems are reviewed in Section II. The set-up of an ARoF system in a shared scenario with a PoF signal used to evaluate the propagation of 5G NR signals including influence of non-linear effects and CD and the set-up to characterize HPL noise are presented in Section III. Next, Section IV includes experimental results and simulations to support them. Finally, Section V presents the conclusions.

## II. Theory

### A. Non-Linear Effects and Noise Transfer

Non-linear effects are a limiting factor when it comes to injecting relatively high-power optical signals into optical fibers. These non-linear effects can be classified in two main groups: Kerr effect-related non-linear effects and scattering-related non-linear effects.

The first group of non-linear effects is divided into Self-Phase Modulation (SPM) effect, Cross-Phase Modulation (XPM) effect and Four-Wave Mixing (FWM) effect. FWM effect is negligible in high dispersive optical fibers. SPM and XPM effects consist of a refractive index variation induced by the electromagnetic fields propagating through an optical fiber. In the first case, the refractive index variation is produced by the data signal itself. By contrast, XPM effect is produced by a multiplexed signal (e.g., a PoF signal). The optical fiber refractive index induced by SPM can be expressed as [18]:

$$n = n_0 + n'|E|^2 \tag{1}$$

where $n_0$ is the linear refractive index, $n'$ is the non-linear refractive index, ($3.2 \times 10^{-16}$ cm$^2$/W for silica fibers) and $E$ is the electric field intensity, respectively. By solving the Schrödinger equation for dispersive and non-linear fibers, the expression for the non-linear phase-shift induced by SPM can be obtained [18]:

$$\phi_{SPM} = \frac{2\pi \cdot n'}{\lambda \cdot A_{eff}} \cdot L_{eff} \cdot |E|^2 \tag{2}$$

where $\lambda$ is the wavelength, $A_{eff}$ is the optical fiber effective area, (80 μm$^2$ for standard SMFs), and $L_{eff}$ is the fiber effective length,respectively. The last is given by [19]:

$$L_{eff} = \frac{1 - e^{-\alpha_p \cdot L}}{\alpha_p} \tag{3}$$

where $\alpha_p$ is the attenuation coefficient and $L$ is the actual optical fiber length.

XPM involves two different optical beams, the expression for overall non-linear induced refractive index is given by [20]:

$$n = n_0 + n'|E_1 + E_2|^2 \tag{4}$$

being $E_1$ and $E_2$ the intensity of both electric fields involved in the XPM effect. Following the same approach as in (2), the overall non-linear induced phase shift is given by [20]:

$$\phi_{NL} = \frac{2\pi \cdot n'}{\lambda \cdot A_{eff}} \cdot L_{eff} \cdot \left(|E_1|^2 + 2|E_2|^2\right) \tag{5}$$

In the expression of the non-linear phase shift above, the XPM term (second) is always accompanied by the SPM term (first).

The second group of non-linear effects includes Stimulated Brillouin Scattering (SBS) and Stimulated Raman Scattering (SRS). These effects manifest themselves as partial reflections of the propagating beam when a certain power level is reached. For SBS, the optical power threshold at which the effect starts to manifest is calculated as [20]:

$$P_{SBS} = \frac{21 \cdot k \cdot A_{eff}}{g_B \cdot L_{eff}} \cdot \frac{\Delta v_B + \Delta v_P}{\Delta v_B} \tag{6}$$

where $g_B$ is the Brillouin gain coefficient, $k = 2$, $\Delta v_B$ is the Brillouin gain bandwidth (35 MHz typically) and $\Delta v_P$ is the pump laser linewidth. The second term indicates that increasing $\Delta v_P$ then increases the power threshold of SBS as well.

The threshold power for SRS is given by [20]:

$$P_{SRS} = \frac{16 \cdot A_{eff}}{g_R \cdot L_{eff}} \tag{7}$$

where $g_R$ is the Raman gain coefficient. If this limit is reached, a part of the energy carried by the high-power signal is scattered, meaning that losses increase and leading to a potential PoF transmission efficiency penalty. For all wavelengths, $g_R \ll g_B$. But the inclusion of a multiplexed high-power optical signal in the system in combination with the laser bandwidth influence on the SBS threshold power can turn SRS into the limiting non-linear effect in shared scenarios. SRS can be beneficial because part of the energy scattered by this effect is transferred to the data signal. This is known as Raman amplification. The Raman gain $G$ is given by [19]:

$$G = exp(g_R P_0 L_{eff} - \alpha_s L_{eff}) \tag{8}$$

where $P_0$ is the pump power, and $\alpha_s$ is the SMF attenuation at signal's wavelength. Another way to analyze Raman amplification is using the ratio between data signal's received power with the HPL turned on and turned off, known as On/Off Raman gain and given by [19]:

$$G_{R\ On/Off} = exp\left(g_R P_0 L_{eff}\right) \tag{9}$$

On the other hand, in shared scenarios where the high-power signal is very noisy, data signal is amplified but also affected by the HPL noise. The noise of a light source can be expressed in terms of the Relative Intensity Noise (RIN) [19]:

$$RIN = \frac{\langle \Delta P^2 \rangle}{P^2} \tag{10}$$

where $\langle \Delta P^2 \rangle$ is the optical power quantum fluctuation of the optical source and $P$ is the mean optical power. In shared scenarios where the high-power signal and data signal, respectively, have significantly different wavelengths, the noise transfer in terms of RIN can be expressed as [19]:

$$RIN_S^0 = RIN_S^i + RIN_P \cdot ln^2 G \cdot \frac{\frac{1}{L_{eff}}}{\alpha_P^2 + (2\pi f_p D \Delta\lambda)^2} \tag{11}$$

where $RIN_S^0$ is the total noise transfer, $RIN_S^i$ is the noise of the data optical source, $RIN_P$ is the noise of the high-power optical source, $G$ is the Raman gain obtained from (8), $f_p$ is the noise frequency of the high-power optical source, $D$ is the CD and $\Delta\lambda$ is the separation between the signal wavelength and the high-power signal wavelength.

### B. Power Fading Effect

When an optical carrier of frequency $f_{opt}$ is modulated by a RF signal of frequency $f_c$, the optical spectrum presents a central tone at a frequency $f_{opt}$ and two sidebands. The separation in frequency between the optical carrier and each sideband is $f_c$. When this signal is transmitted through an optical fiber, CD causes a propagation speed difference that ultimately leads to a phase shift between both sidebands. Those sidebands are mixed at the photodetector, creating constructive or destructive interferences. This chromatic-induced power fading is described by modeling the optical fiber as a band-pass filter with the following expression [21],

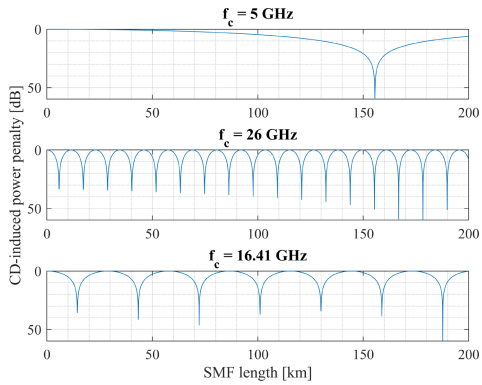


Fig. 1. CD-induced power penalty as a function of the SMF length for different RF frequency, $f_c$. $\lambda = 1552.8$ nm, $D = 16$ ps/nm/km.

$$H(f) = e^{-i\alpha f^2} \tag{12}$$

$$\alpha = \pi D \frac{\lambda^2}{c} L \tag{13}$$

where $c$ is the speed of light and $f$ is the frequency difference between the optical carrier and each sideband (i.e., $f_c$). One way to study this effect in complex signals (e.g. 5G NR signals) is by measuring the received electrical spectrum power after traveling through a SMF, $P_{prop.}$, and comparing it to the power received in a back-to-back (B2B) scenario, $P_{B2B}$. The ratio between both values is called power penalty, and expressed in dB is given by:

$$PowerPenalty[dB] = P_{B2B}[dBm] - P_{prop.}[dBm] \tag{14}$$

This is equivalent to the Carrier-to-Noise (C/N) penalty used in [21]. The destructive interference between both sidebands, or signal extinction, is maximum when the phase shift generated by the CD between each sideband and the optical carrier is $\pi/2$ radians. Therefore, the value of $f_c$ at which the signal extinction and power penalty is maximum, which is called the critical frequency, is given by [21]:

$$\alpha f_c^2 = \frac{\pi}{2} \rightarrow f_c = \sqrt{\frac{c}{2D\lambda^2 L}} \tag{15}$$

Using (12) and (13) implemented in Matlab, the CD-induced power fading as a function of the SMF length is simulated and shown in Fig. 1 for specific RF carrier frequencies. The RF carrier frequencies of 5 GHz and 26 GHz are within the 5G NR frequency bands. 5 GHz is stablished in the Frequency Range (FR) 1 and 26 GHz is stablished in the FR2. The RF carrier frequency of 16.41 GHz is the critical frequency corresponding to a 14.43 km long SMF, which is the one used in the experiments as described next.

The simulations show a similar behavior around the critical length for each RF frequency and vice versa. The limitations on

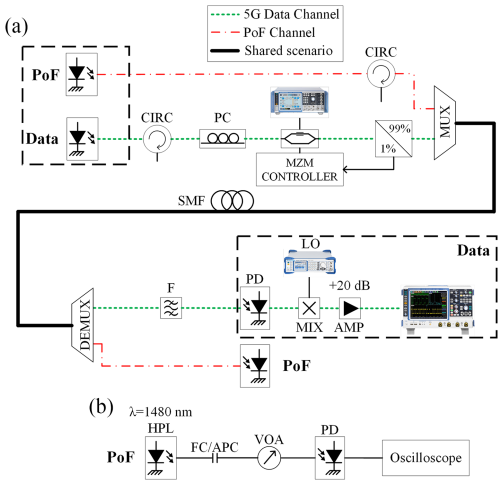


Fig. 2. Experimental setups: (a) Non-linear effects and ARoF 5G NR transmission. (b) HPL characterization. CIRC: Circulator, PC: Polarization Controller, MUX: Multiplexer, DEMUX: Demultiplexer, F: Filter, MIX: Mixer, LO: Local Oscillator, AMP: RF Amplifier, PD: Photodiode, VOA: Variable Optical Attenuator, HPL: High Power Laser.

the reception equipment's bandwidth used in the experiments determines the selection of the RF carrier frequencies used to measure the CD-power fading, close but not included in the 5G NR frequency bands. Nevertheless, the results obtained from the experiments can be used to extrapolate the behavior of more realistic 5G NR links.

## III. Experimental Setup

The main experimental setups are presented in Fig. 2. A $\lambda_D$ = 1552.8 nm laser diode (LD) is externally modulated by an *Optilab IMC-1550-20-PM* Mach-Zehnder Modulator (MZM) controlled by a *PlugTech PowerBoard* MZM controller. The optical power of the LD is set to $P_{in\_D}$ = +5 dBm for all the measurements. The wavelength of the LD was experimentally measured using a *Yokogawa AQ6370D* Optical Spectrum Analyzer (OSA). The electrical signal to modulate the optical carrier is generated by the *SMW200 A* Vector Signal Generator (VSG). This signal consists of an up-to 20 GHz RF carrier modulated with a standardized 5G NR baseband signal. The modulated optical signal is multiplexed with a $\lambda_P$ = 1480 nm PoF signal generated by a *Keopsys CRFL-02-1480* HPL with a maximum output power of $P_{in\_P}$ = +33 dBm and a linewidth of 2 nm, which is wide enough to make SBS a non-determining factor in the experiments. Both optical sources are protected using optical circulators that, in addition, allow us to measure the backscattered power. Both signals are transmitted through a standard SMF of variable lengths depending on the experiment performed. The lengths of all the SMFs were directly measured with a *EXFO FTB-1* Optical Time Domain Reflectometer and, since the SMF datasheet only provides a maximum CD value, CD was also obtained from (15) by measuring the critical frequency of the SMF. The PoF signal and the data signal are then separated using a demultiplexer. The PoF signal is connected to a *Coherent PM30* high-power photodiode (PD) to measure its power, and the data signal is filtered with an optical filter centered at 1550 nm and

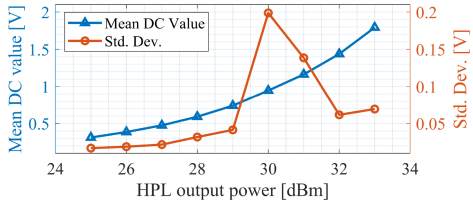


Fig. 3. Measurements of average value and standard deviation for the HPL.

detected using a *Discovery Semiconductors DSC30S* high-speed PD. In the electrical domain, a *Mini-Circuits ZX05-24MH-S+* mixer and a *Rohde & Schwartz SMB100 A* local oscillator (LO) are used to down-convert the carrier frequency and place it within the BW of the *Rohde & Schwartz RTO1022* oscilloscope, which is 2 GHz. This oscilloscope is connected to the *Rohde & Schwartz Vector Signal Explorer software*, which is a Vector Signal Analyzer (VSA) that can measure different parameters of the transmitted 5G NR signal. In this work, the power penalty defined in Section II and the Error Vector Magnitude (EVM) are the two parameters used to evaluate the quality of the received data.

Additionally, a secondary experiment to measure the behavior of the HPL was implemented. In this case, the output of the HPL is measured using a PD and a Variable Optical Attenuator (VOA) to prevent the PD from saturation. The output of the PD is connected to an oscilloscope to measure the average voltage and the noise detected.

## IV. Simulations and Experimental Results

In this section, a characterization of the main effects that can affect both the 5G NR and the PoF signals will be carried out. The HPL behavior and the non-linear effects arouse by the PoF signal will be evaluated. Moreover, the transmission of different 5G NR signals in a shared scenario will be analyzed.

### A. HPL Characterization

In Raman lasers like the one characterized in this section, a noisy behavior is common. For certain powers, resonant cavities can appear, giving rise to transverse modes instabilities and, ultimately, non-desired tones in the optical signal [17]. Thus, the behavior of the HPL was analyzed using the setup of Fig. 2(b). The HPL output power was swept from +25 dBm to +33 dBm in steps of 1 dBm, and the average value and standard deviation of the voltage after detection was analyzed. Fig. 3 shows the results. The average value of the detected voltage follows an exponential curve, but the noise of the HPL increases when the optical power is set close to 30 dBm. Therefore, when the HPL output power is set at around 30 dBm, data signal can be affected due to noise transfer.

### B. Non-Linear Effects Characterization

The PoF signal transmission efficiency was evaluated. To do so, the setup shown in Fig. 2(a) was slightly modified. The detection stage for the data signal (framed with a dashed line in

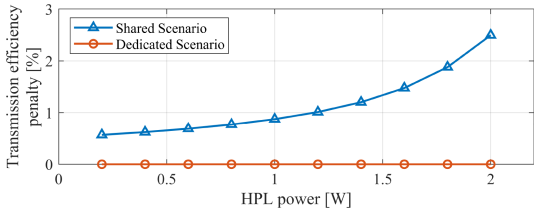


Fig. 4. Simulations of transmission efficiency penalty in a 14.43 km SMF vs HPL power.

Fig. 2(a)) was replaced by a power meter and the 5G NR modulation was deactivated in order to have a stable CW optical power measurement. The rest of the system remained unchanged. Losses of the PoF signal were measured for HPL powers of $P_{in\ P}$ = +27 dBm and $Pi_{n\ P}$ = +33 dBm, with almost no difference between them, meaning that SRS effect on PoF transmission is very small. If the HPL is set at +33 dBm and is co-transmitted with the data signal of 5 dBm at 1552.8 nm, there is an imperceptible penalty in the PoF transmission efficiency due to Raman amplification. We also simulated different scenarios with VPIphotonics software tool: a dedicated scenario where only the HPL signal is transmitted; and a shared scenario where the HPL signal is transmitted along with the +5 dBm 1552.8 nm data signal. The HPL output power was swept from 200 mW to 2 W and injected in a 14.43 km SMF link. A Raman gain profile for 1486 nm [22] was used in these simulations. Results of PoF transmission efficiency penalty on the shared scenario are shown in Fig. 4. In dedicated scenario, the transmission efficiency penalty induced by non-linear effects is very close to 0%. In shared scenario, the transmission efficiency penalty increases with the HPL power. The maximum transmission efficiency penalty is 2.49% for a HPL power of 2 W, which means that 49.8 mW are transferred to the data signal due to Raman amplification. This is a very small penalty in the high-power transmission efficiency and, therefore, we considered it negligible. If we add the transferred power to the LD power, the On/Off Raman gain results in 12.44 dB, which is similar to the On/Off Raman gain measured in the experiments presented next (12.7 dB for a HPL power of 2 W).

The On/Off Raman gain in the data channel generated by the high-power signal was also analyzed. First, the optical power received at 1552.8 nm was measured for six different cases: for the HPL turned OFF and for HPL powers +27 dBm, +28 dBm, +30 dBm, +32 dBm and +33 dBm. Then, the On/Off Raman gain was simulated in VPIphotonics software where two equivalent optical fibers were used to transmit different signals. Through the first one, the 1552.8 nm signal and the PoF signal were multiplexed and transmitted in a shared scenario. In the second one, only the 1552.8 nm signal was transmitted. At the output of both SMFs, the optical signal was filtered and the 1552.8 nm optical power was detected. The ratio between both optical powers corresponds to the On/Off Raman gain. The HPL output power was swept from +23 dBm to +33 dBm in steps of 0.1 dBm for this simulation, see Fig. 5.

There is a good agreement between simulations and experimental results. For example, at a HPL output power of +27 dBm the simulated On/Off Raman gain was 3.03 dB whereas 12.37 dB

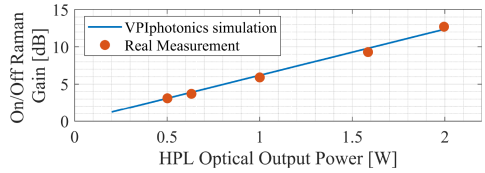


Fig. 5. On/Off Raman gain simulations and measurements (circles). $\lambda_D$ = 1552.8 nm, $\lambda_P$ = 1480 nm, $L$ = 14.43 km, $P_{in\_D}$ = +5 dBm.

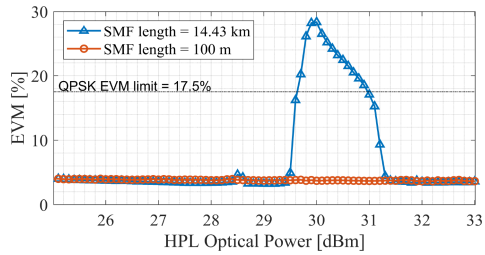


Fig. 6. Measurements of 5G NR signal's EVM vs HPL injected optical power after 14.43 km. $\lambda_D$ = 1552.8 nm, $\lambda_P$ = 1480 nm, $L$ = 14.43 km, $P_{in\_D}$ = +5 dBm, RF frequency = 10 GHz, RF power = +10 dBm.

for a HPL output power of +33 dBm, quite similar to 3.1 dB and 12.7 dB obtained from the experiments (represented by the red circles in Fig. 5).

### C. HPL Noise Transfer to 5G NR Data

We measured the effect of the HPL noise in the 5G NR data signal transmitted through 100 m and 14.43 km-long SMFs links with the setup depicted in Fig. 2(a). The baseband signal was a QPSK 5G NR signal which is standardized by 3GPP in the 5G NR protocol. The RF carrier was set at 10 GHz with +10 dBm of RF power. We selected a carrier frequency of 10 GHz because it is far away from the critical frequency in both cases, allowing us to analyze the effect of HPL noise transfer in a clear 5G NR signal at all link lengths. To evaluate the quality of the 5G NR signal, its EVM was measured at different HPL powers ranging from +25 dBm to +33 dBm in steps of 0.1 dBm, and then compared to the limit set by the 5G NR standard, which is 17.5%, see Fig. 6. At a 100 m SMF link, the EVM of the received signal remains constant for all the HPL powers tested, which means that negligible noise transfer occurs at this length. When the SMF length increases, the noise transfer from the PoF signal to the data signal becomes more noticeable. In a 14.43 km SMF link, when the HPL power is set at +30 dBm, the measured EVM exceeds the limit set by the 5G NR 3GPP standard. In (11), which describes the noise transfer happening in a SMF, $G$ grows more than $L_{eff}$ with SMF length. This is the reason why noise transfer is negligible for short SMF and becomes noticeable for longer SMF distances.

In [23], a 5 km-long SMF link is tested for a 16QAM 5G NR signal for the same HPL and in a similar setup to the one used in this work. The measured EVM was 12.5% for a HPL power of $P_{in\_P}$ = +30 dBm. The HPL noise transfer is identified as a relevant impairment as the link length increases due to SRS. For this reason, no HPL output powers around +30 dBm will be used in the next measurements.

TABLE I
LIST OF 5G NR SIGNALS USED IN SIMULATIONS AND EXPERIMENTS

| MODULATION FORMAT | SCS [kHz] | Baseband BW [MHz] |
|---|---|---|
| QPSK | 30 | 5 |
| | 60 | 10, 20, 30, 40, 50, 60, 70, 80, 90, 100, 200 |
| | 120 | 400 |

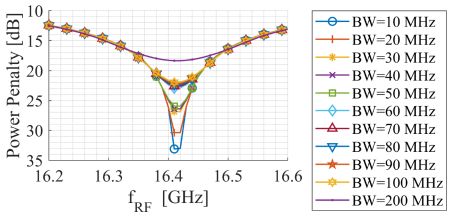


Fig. 7. Simulations of the CD-induced power penalty for 5G NR baseband signals with different BWs. $\lambda_D = 1552.8$ nm, CD = 16 ps/nm/km.

### D. Power Fading and PoF in 5G NR Data

The CD-induced power fading for different conditions was also simulated and measured. The effect of including a PoF signal was also checked. First, a number of simulations were carried out using an ad-hoc software developed in Matlab and Simulink tools. This software was designed to calculate the transfer function of a SMF using (12) and (13). Then, the baseband signals used in the real experiment, which are listed in Table I, were generated with the *5G Waveform Generator* toolbox. These 5G NR signals are used to modulate an RF carrier ranging from 15 GHz to 17 GHz. The simulation of the power penalty due to CD-induced power fading calculated with (14) is shown in Fig. 7. For all the simulations, the SMF length was set to 14.43 km, which is the length of the SMF used in the experiment described next. The simulations showed that the power fading is maximum at a carrier frequency of 16.43 GHz (critical frequency). The simulations also showed that, for higher 5G NR baseband bandwidths, the maximum power penalty decreases. An additional simulation keeping the baseband BW constant and changing the subcarrier spacing (SCS) was carried out. No influence of the SCS on the maximum power penalty of the 5G NR signal was observed. Since these simulations are performed without considering noise, specific maximum power penalty values obtained are not to be directly extracted from these simulations or compared to the experimental results presented next. The rest of the simulation results can be compared.

Next, the experiment was carried out with a 14.43 km-long SMF link. This length was chosen so that the maximum power penalty is within the VSG range. The RF carrier frequency was swept from 15.5 GHz to 17.5 GHz in steps of 10 MHz and the power of the 5G NR signal was measured. This test was done for some of the 5G NR signals listed in Table I.

Back-to-back measurement without SMF was performed, measuring the power of the 5G NR signal's spectrum for each RF carrier frequency. Next, the 14.43 km SMF was placed and the received 5G NR signal's spectrum power was measured

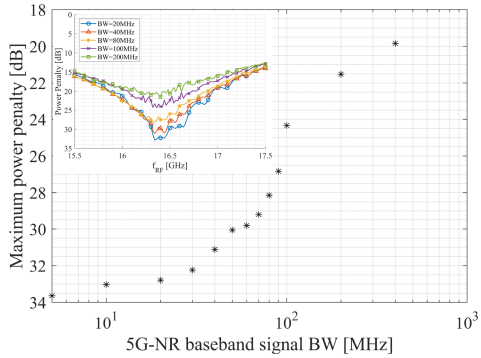


Fig. 8. Measurements of the maximum power penalty vs 5G NR baseband signal BW. Inset: Power penalty vs RF carrier frequency for different baseband signal BWs.

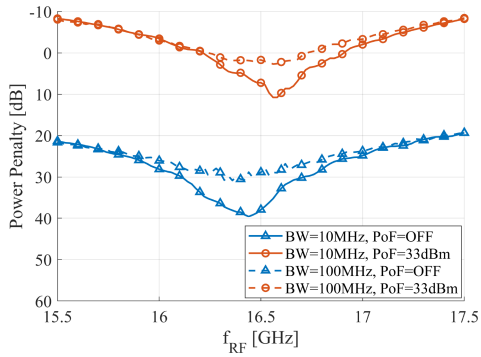


Fig. 9. Measurements of power penalty vs RF carrier frequency for different 5G NR baseband signal BWs and for different HPL powers.

once again. As shown in (14), power penalty is calculated by substracting the received spectrum power to the B2B spectrum power. Fig. 8 shows the maximum power penalty measured for each 5G NR signal tested. Its inset depicts the power penalty of each signal as a function of the RF carrier frequency. The measurements show that power penalty is smaller when baseband signal BW increases, in good agreement with the simulations. This is due to the relative narrowness of the SMF band-pass filtering effect. When baseband signal BW increases, the filter only induces losses to part of the signal. The higher the BW, the smaller the affected area will be with respect to the total baseband signal BW. If total powers from received and B2B spectrums are calculated and subtracted, the difference will be smaller for higher baseband BW.

Then, PoF signal was added. The baseband BWs selected for this test were 10 MHz and 100 MHz, with a SCS of 60 kHz in both cases. Two different measurements were carried for different HPL conditions (OFF and +33 dBm of output power). Results are shown in Fig. 9. When the PoF signal is included in the experiment the power fading becomes smaller because of Raman amplification in the SMF. When the HPL output power is set to +33 dBm and the BW of the 5G NR baseband signal is set to 100 MHz, the power penalty is close to 0 dB for the critical frequency, and for the rest of the carrier frequencies a gain in the 5G NR signal's spectrum can be measured. Additionally, a shift in the critical frequency of 100 MHz when the HPL is set to

TABLE II
MEASURED MAXIMUM POWER PENALTY IMPROVEMENT IN THE ELECTRICAL DOMAIN

| SCS [kHz] | Baseband BW [MHz] | HPL Power [dBm] | Power Penalty Improvement [dB] |
|---|---|---|---|
| 60 | 10 | 33 | 28.79 |
| | 100 | 33 | 27.95 |

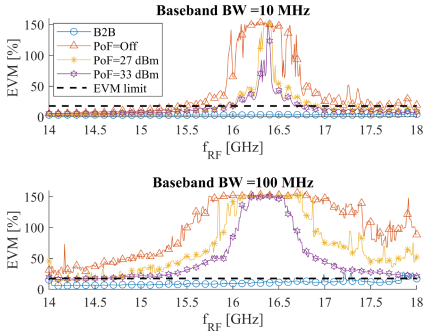


Fig. 10. 5G NR signal's EVM in B2B scenario and after 14.43 km SMF for HPL Off, +27 dBm, +33 dBm. Top: Baseband BW = 10 MHz, Bottom: Baseband BW = 100 MHz.

+33 dBm can be observed, which is produced by the SPM and XPM-induced phase shift on the transmitted signal (described with (2) and (5)). This phase shift is opposite to the one induced by CD, extracted from (12). Therefore, it can be said that SPM and XPM partially compensate for the CD-induced phase shift on the transmitted optical signal. Critical frequency shifts were also measured for other SMF lengths, and for longer distances the shift was found to be greater. For example, for a 25.2 km long SMF link (from all available SMF lengths in our laboratory, the one causing the largest critical frequency shift in current set-up), the shift measured in the critical frequency was 250 MHz. XPM influence in ARoF links is briefly discussed in [24], however its critical frequency shift was not measured and no analysis of the baseband BW effect was provided. Table II summarizes the effect of PoF on the power penalty on the data signal. The EVM of the 5G NR received signal was also measured for 5G NR signals with baseband BWs of 10 MHz and 100 MHz, and for HPL output powers of +27 dBm, +33 dBm. Results are shown in Fig. 10. The measurements show that, even though power penalty is weaker for higher baseband BWs, the EVM of the received signal worsens dramatically when the baseband BW increases. As an example, at a RF carrier frequency of 15 GHz, the EVM of the received signal at a baseband BW of 10 MHz was 11.3%. If the baseband BW is increased to 100 MHz, the EVM of the detected signal reaches 55%. The experiment also showed that the inclusion of a PoF signal is beneficial for the transmitted 5G NR signal quality. For a baseband BW of 10 MHz and a 17 GHz RF carrier frequency, if the HPL is OFF, the EVM exceeded the limit set by the 5G NR standard. However, if the HPL was turned on, the EVM decreased to 14.3% for +27 dBm and 11.6% for +33 dBm, respectively. Both values are within the limits of the 5G NR standard. Fig. 11 presents a summary of the results.

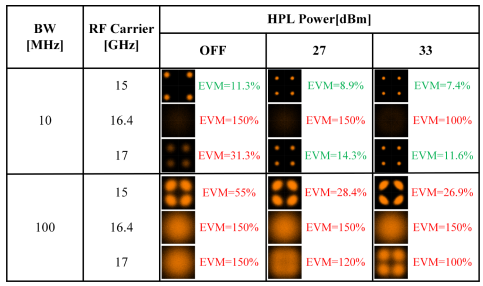


Fig. 11. Constellations and EVM measurements for different 5G NR baseband BWs and HPL output powers. $\lambda_D = 1552.8$ nm, L = 14.43 km.

## V. CONCLUSION

In this work, the influence of non-linear effects caused by PoF signals as well as the impact of CD on the transmission of 5G NR signals in ARoF systems was discussed, simulated, and experimentally tested.

SRS effect has a negligible influence on the PoF transmission efficiency for the HPL powers tested when the 1552.8 nm LD is either activated or deactivated. However, the EVM of the 5G NR signal was dramatically penalized at long SMF lengths when the HPL output power was close to +30 dBm because of the SRS non-linear effect and the noise transfer from the PoF signal to the 5G NR signal.

The chromatic-induced power fading effect was measured for 5G NR signals with different baseband bandwidths (BWs) finding that, for higher baseband BWs, the power fading smoothed and the power of the detected electrical spectrum increased. However, the 5G NR signal quality worsened for higher baseband BWs.

The influence of the PoF signal was also analyzed for 5G NR signals with baseband BWs of 10 MHz and 100 MHz. A power penalty improvement of over 27 dB was measured for both baseband BWs and a HPL output power of +33 dBm. A shift in the power fading critical frequency of 100 MHz for a link length of 14.43 km and 250 MHz for a link length of 25.2 km were measured when using a +33 dBm HPL output power. The results also showed that the PoF signal improves the EVM of the 5G NR signal to make it compliant with the 3GPP standard in some cases because of the Raman gain. For a 5G NR baseband signal BW of 10 MHz and a RF carrier frequency of 17 GHz, the EVM improves from 31.3% to 11.6% for a HPL output power of +33 dBm.

## REFERENCES

[1] C. Ranaweera, J. Kua, I. Dias, E. Wong, C. Lim, and A. Nirmalathas, "4G to 6G: Disruptions and drivers for optical access [Invited]," *J. Opt. Commun. Netw.*, vol. 14, no. 2, pp. A143–A153, Feb. 2022.
[2] X. Liu, "Enabling optical network technologies for 5G and beyond," *J. Lightw. Technol.*, vol. 40, no. 2, pp. 358–367, Jan. 2022.
[3] C. J. Bernardos and M. A. Uusitalo, "European vision for the 6G network ecosystem," Zenodo, Tech. Rep., Jun. 2021, doi: 10.5281/zenodo.5007671.
[4] P. Rost et al., "Cloud technologies for flexible 5G radio access networks," *IEEE Commun. Mag.*, vol. 52, no. 5, pp. 68–76, May 2014.
[5] S. Rommel et al., "Towards a scaleable 5G fronthaul: Analog radio-over-fiber and space division multiplexing," *J. Lightw. Technol.*, vol. 38, no. 19, pp. 5412–5422, Oct. 2020.

[6] D. S. Montero, J. López-Cardona, F. M. A. Al-Zubaidi, I. Pérez, P. C. Lallana, and C. Vázquez, "The role of power-over-fiber in C-RAN fronthauling towards 5G," in *Proc. 22nd Int. Conf. Transparent Opt. Netw.*, 2020, pp. 1–4.
[7] J. D. Lopez-Cardona, R. Altuna, D. Sanchez Montero, and C. Vazquez, "Power over fiber in C-RAN with low power sleep mode remote nodes using SMF," *J. Lightw. Technol.*, vol. 39, no. 15, pp. 4951–4957, 2021.
[8] H. Yang et al., "10-W power light co-transmission with optically carried 5G NR signal over standard single-mode fiber," *Opt. Lett.*, vol. 46, no. 20, pp. 5116–5119, Oct. 2021.
[9] C. Vázquez et al., "Multicore fiber scenarios supporting power over fiber in radio over fiber systems," *IEEE Access*, vol. 7, pp. 158409–158418, 2019.
[10] J. D. López-Cardona et al., "Power-over-fiber in a 10 km long multicore fiber link within a 5G fronthaul scenario," *Opt. Lett.*, vol. 46, no. 21, pp. 5348–5351, Nov. 2021.
[11] T. Umezawa et al., "100-GHz fiber-fed optical-to-radio converter for radio- and power-over-fiber transmission," *IEEE J. Sel. Topics Quantum Electron.*, vol. 23, no. 3, pp. 23–30, May 2017.
[12] J. D. López Cardona, P. C. Lallana, R. Altuna, A. Fresno-Hernández, X. Barreiro, and C. Vázquez, "Optically feeding 1.75 W with 100 m MMF in efficient C-RAN front-hauls with sleep modes," *J. Lightw. Technol.*, vol. 39, no. 24, pp. 7948–7955, Dec. 2021.
[13] L. C. d. Souza, E. S. Lima, and A. C. S. Junior, "Implementation of a full optically-powered 5G NR fiber-wireless system," *IEEE Photon. J.*, vol. 14, no. 1, pp. 1–8, Feb. 2022.
[14] M. Matsuura, H. Nomoto, H. Mamiya, T. Higuchi, D. Masson, and S. Fafard, "Over 40-W electric power and optical data transmission using an optical fiber," *IEEE Trans. Power Electron.*, vol. 36, no. 4, pp. 4532–4539, Apr. 2021.
[15] F. M. A. Al-Zubaidi, D. S. Montero, and C. Vázquez, "SI-POF supporting power-over-fiber in multi-gbit/s transmission for in-home networks," *J. Lightw. Technol.*, vol. 39, no. 1, pp. 112–121, Jan. 2021.
[16] H. Sotobayashi and K. Kitayama, "Cancellation of the signal fading for 60 GHz subcarrier multiplexed optical DSB signal transmission in nondispersion shifted fiber using midway optical phase conjugation," *J. Lightw. Technol.*, vol. 17, no. 12, pp. 2488–2497, Dec. 1999.
[17] B. Yang et al., "High power monolithic tapered ytterbium-doped fiber laser oscillator," *Opt. Exp.*, vol. 27, no. 5, pp. 7585–7592, Mar. 2019.
[18] F. Ramos, J. Marti, V. Polo, and J. Fuster, "On the use of fiber-induced self-phase modulation to reduce chromatic dispersion effects in microwave/millimeter-wave optical systems," *IEEE Photon. Technol. Lett.*, vol. 10, no. 10, pp. 1473–1475, Oct. 1998.
[19] H. Clifford and P. Agraval, *Raman Amplification in Fiber Optical Communication Systems*, 1st ed. New York, NY, USA: Academic Press, 2005.
[20] J. Toulouse, "Optical nonlinearities in fibers: Review, recent examples, and systems applications," *J. Lightw. Technol.*, vol. 23, no. 11, pp. 3625–3641, Nov. 2005.
[21] U. Gliese, S. Norskov, and T. Nielsen, "Chromatic dispersion in fiber-optic microwave and millimeter-wave links," *IEEE Trans. Microw. Theory Techn.*, vol. 44, no. 10, pp. 1716–1724, Oct. 1996.
[22] S. Aleksic, F. Hipp, D. Winkler, A. Poppe, B. Schrenk, and G. Franzl, "Perspectives and limitations of QKD integration in metropolitan area networks," *Opt. Exp.*, vol. 23, no. 8, pp. 10359–10373, 2015.
[23] F. M. A. Al-Zubaidi, J. D. López Cardona, D. S. Montero, and C. Vázquez, "Power-over-fiber impact on 5G NR transmission in standard single mode fibers," in *Proc. Int. Topical Meeting Microw. Photon.*, 2021, pp. 1–4.
[24] F. M. A. Al Zubaidi, J. D. López Cardona, D. S. Montero, and C. Vázquez, "Optically powered radio-over-fiber systems in support of 5G cellular networks and IoT," *J. Lightw. Technol.,* vol. 39, no. 13, pp. 4262–4269, 2021.

**Rubén Altuna** received the M.Sc. degree in electronics systems engineering in 2020 from the Universidad Carlos III of Madrid, Spain, where he is currently working toward the Ph.D. degree in electrical, electronics and automation engineering. His research interests include radio over fiber, multicore optical fibers, instrumentation, and power over fiber systems.

**J. D. López-Cardona** received the M.Sc. degree in electronics systems engineering from the Universidad Carlos III of Madrid, Spain, in 2016, and the Ph.D. degree in electrical, electronics and automation engineering in 2022. His research interests include low power electronics, biomedical applications, multicore optical fibers, low power electronics, and power over fiber systems.

**Fahad M. A. Al-Zubaidi** received the M.Sc. degree in laser and communication engineering from the University of Baghdad, Baghdad, Iraq, in 2015, and the Ph.D. degree in electrical, electronics and automation engineering from the Department of Electronics Technology from the Universidad Carlos III of Madrid, Spain, in 2021. His research interests include plastic optical fibers, 5G cellular networks, radio over fiber, and power over fiber systems.

**D. S. Montero** received the Ph.D. degree in electrical, electronics and automation engineering from the Department of Electronics Technology, the Universidad Carlos III of Madrid (UC3M), Spain, in 2011. He is currently an Associate Professor with the Department of Electronics Technology, UC3M. His research interests include fiber-optic sensors, multicore optical fibers, WDM-PON networks, and power over fiber systems.

**Carmen Vázquez** (Senior Member, IEEE) received the Ph.D. degree in Photonics from the Telecommunications Engineering School, Polytechnic University of Madrid, Spain, in 1995. From 1992 to 1995, she was with Optoelectronics Division, Telefónica Investigación y Desarrollo. She was involved in III-V integrated optics devices characterization, design, and fabrication. In 1995, she joined UC3M where she is currently a Full Professor and the Head of the Displays and Photonic Applications Group. She was Visiting Scientist with the Research Laboratory of Electronics, Massachusetts Institute of Technology, MA, USA, from 2012 to 2013, working on silicon photonics. Her research interests include integrated optics, optical communications and instrumentation, including, plastic and multicore optical fibers, broadband access networks and monitoring techniques, RoF systems, power over fiber, fiber optic sensors, and 5G & WDM networks. She was the recipient of a Fellowship with TELECOM, Denmark, in 1991, working on erbium-doped fiber amplifiers. She was leading principal investigator on PoF at BlueSPACE (Building on the Use of Spatial Multiplexing 5G Networks Infrastructures and Showcasing advanced technologies and Networking Capabilities) and now coordinates 6G-Xtreme project. She is a Fellow of SPIE.